S31A-1898: Exploiting head-wave artifacts in seismic interferometry

Dylan Mikesell*, Kasper van Wijk*, Josh Nichols† and Alex Calvert‡

*Physical Acoustics Lab and Department of Geosciences, Boise State University, 1910 University Dr., Boise, ID 83725
† Western GECO 10001 Richmond Avenue Houston, TX 77042
‡ Maersk Oil, A.P. Moller- Maersk A/S Esplanaden 50 1098 Copenhagen K Denmark – formerly at ION - GX Technology, 225 E. 16th Ave., Suite 1200, Denver, CO 80203

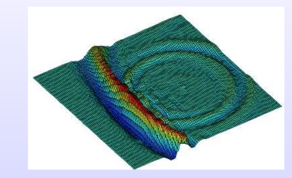

Abstract

We present a novel method to extract subsurface information from spurious head-wave arrivals in seismic interferometry (SI). Wavefields recorded at two receivers are crosscorrelated to generate new data as if one of the receivers was a source. In field applications, some of the acquisition requirements necessary in SI are not met, leading to wavefields containing non-physical artifacts–in our case, a virtual refraction. This particular artifact contains useful information about the subsurface, and we use semblance analysis in the crosscorrelation domain to help us estimate the top layer velocity and thickness.

Seismic interferometry

The Green's function between two receivers is obtained by crosscorrelating the recorded wavefields from sources located on an enclosing surface around the receivers (*Wapenaar and Fokkema*, 2006). In exploration seismics, this technique is often called seismic interferometry (SI). In field data applications we make the following assumptions when applying SI.

- All sources lie in the far-field (i.e., the distance from the source to the receivers and scatterers is large compared to the wavelength).
- Rays take off approximately normal from the integration surface S.
- The medium outside the integration surface S is homogeneous, implying that no energy going outward from the surface is scattered back into the system.
- The medium locally around a source is smooth (the high frequency approximation).

Following these assumptions, the approximate SI integral is equation 31 in *Wapenaar and Fokkema* (2006):

$$\hat{G}(\mathrm{x}_A,\mathrm{x}_B,\omega)+\hat{G}^*(\mathrm{x}_A,\mathrm{x}_B,\omega)\approx\oint_S\frac{2\hat{G}^*(\mathrm{x}_A,\mathrm{x},\omega)\hat{G}(\mathrm{x}_B,\mathrm{x},\omega)}{\rho(\mathrm{x})c(\mathrm{x})}dS.$$

This is the far-field approximated version, requiring only monopole sources in the integral. Figure 1 illustrates this concept for a homogeneous medium with a single scatterer following an experiment by *Snieder et al.* (2008). The numerical data are modeled using the spectral element method (*Komatitsch and Vilotte*, 1998).

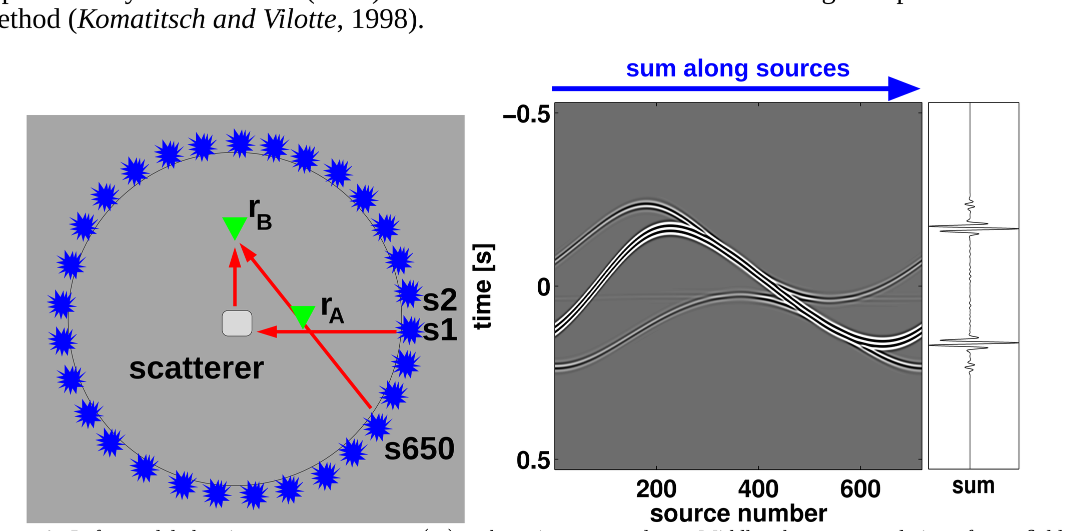

Figure 1: Left: model showing scatterer, sources (s_I) and receivers r_A and r_B. Middle: the crosscorrelation of wavefields at r_A and r_B for each source. The crosscorrelation gather contains events related to the crosscorrelations of the direct and scattered waves. When we sum over sources, we obtain an accurate Green's function with correct direct and scattered arrivals (right).

We replace the single scatterer by a scattering interface and add an array of receivers. The model is shown in Figure 2. After crosscorrelating and summing over sources for each receiver, we create the virtual shot record on the right. The virtual refraction is visible in the new shot record, coming from the correlation of refracted waves at each receiver.

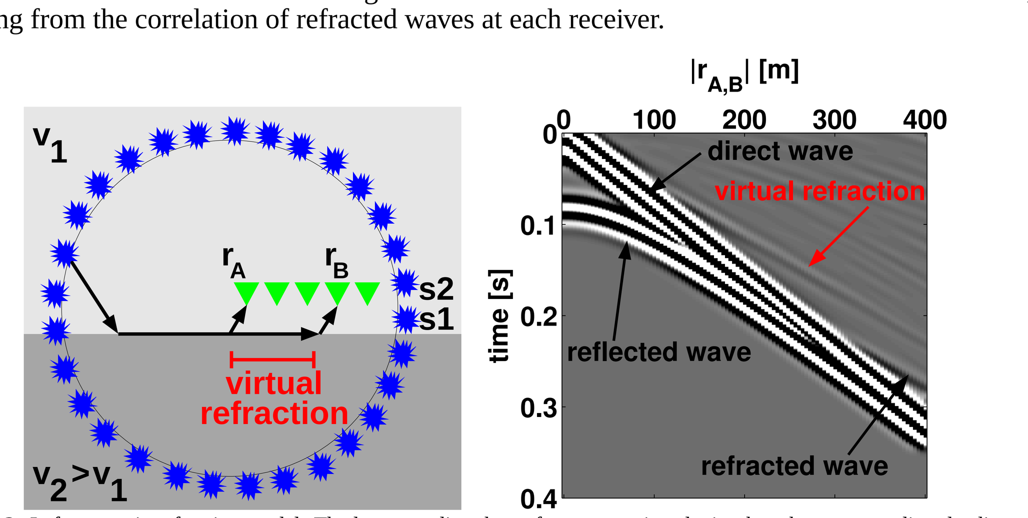

Figure 2: Left: acoustic refraction model. The lower medium has a faster acoustic velocity than the upper medium leading to head-waves for sources past the critical offset. Right: the virtual shot record–the refraction artifact is denoted in red.

The critical offset

The critical offset

$$\sin(\theta_c)\equiv\frac{v_1}{v_2}=\frac{x_c/2}{\sqrt{(x_c/2)^2+H^2}}\Leftrightarrow x_c=\frac{2v_1H}{\sqrt{v_2^2-v_1^2}}$$

is equal to the location of a stationary-phase point in the crosscorrelation related to the travel time difference between the reflected wave at r_A and the refracted wave at r_B (*Mikesell et al.*, 2009).

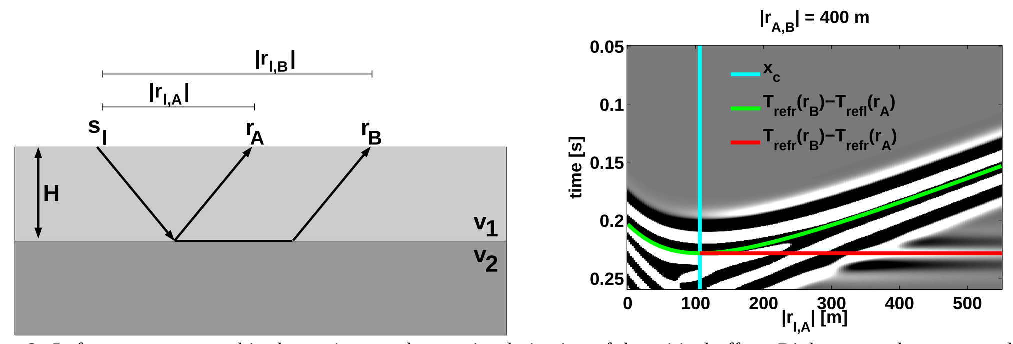

Figure 3: Left: parameters used in the stationary-phase point derivation of the critical offset. Right: example crosscorrelation gather from the receiver at 400 m offset in Figure 2. The critical offset is identified by the extremum of T_{xcor}.

The travel time difference curve (T_{diff}) associated with the critical offset in the crosscorrelation domain is given by $T_{diff}=T_{refr}(r_B)-T_{refl}(r_A)$, where

$$T_{refl}(r_A)=\sqrt{\frac{|r_{I,A}|^2}{v_1}+\frac{2H^2}{v_1}}\ \text{ and }\ T_{refr}(r_B)=\frac{2H\cos\theta_c}{v_1}+\frac{|r_{I,B}|}{v_2}.$$

The source number is I and we can rewrite the term $|r_{I,B}|$ as $|r_{I,A}+r_{A,B}|$. Substituting this term into $T_{refr}(r_B)$ we get

$$T_{diff}=T_{refr}(r_A)-T_{refl}(r_A)+\frac{|r_{A,B}|}{v_2}.$$

The stationary-phase point associated with the minimum of T_{diff} is found by setting the derivative equal to zero and solving for $|r_{I,A}|$.

$$\frac{d}{dr_{I,A}}\left(T_{refr}(r_A)-T_{refl}(r_A)+\frac{|r_{A,B}|}{v2}\right)=0\ \Leftrightarrow$$

$$\frac{d}{dr_{I,A}}\left(\left(\frac{2H\cos\theta_c}{v_1}+\frac{|r_{I,A}|}{v_2}\right)-\sqrt{\left(\frac{|r_{I,A}|}{v_1}\right)^2+\left(\frac{2H}{v_1}\right)^2}+\frac{|r_{A,B}|}{v2}\right)=0\ \Leftrightarrow$$

$$\frac{1}{v_2}-\frac{|r_{I,A}|}{v_1\sqrt{|r_{I,A}|^2+(2H)^2}}=0\ \Leftrightarrow\ |r_{I,A}|=\frac{2v_1H}{\sqrt{v_2^2-v_1^2}}=x_c.$$

Semblance analysis

Because we know T_{diff} we apply a crosscorrelation domain semblance technique (*King et al.*, 2010) to estimate the upper layer velocity and thickness. We calculate T_{diff} for various combinations of velocity (v_1) and thickness (H)–taking velocity v_2 from the slope of the virtual refraction. We plot three of these curves in the left plot of Figure 5. We define semblance as

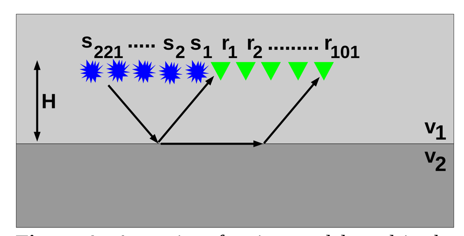

Figure 4: Acoustic refraction model used in the following section. Source increment is 2.5 and receiver increment is 4 m.

$$S=\sum_{i=v_{1,min}}^{v_{1,max}}\sum_{j=h_{min}}^{h_{max}}\frac{E^{out}_{i,j}}{N\times E^{in}_{i,j}},$$

where N equals the number of sources in the crosscorrelation gather. The numerator and denominator are the output energy (E^{out}) and the input energy (E^{in}) defined as

$$E^{out}_{i,j}=\sum_{t(k)=\delta t-t/2}^{\delta t+t/2}\left(\sum_{l=1}^{N}f_{i,j,l,t(k)}\right)^2\ \text{ and }\ E^{in}_{i,j}=\sum_{t(k)=\delta t-t/2}^{\delta t+t/2}\left(\sum_{l=1}^{N}f^2_{i,j,l,t(k)}\right),$$

where f is the crosscorrelation function between two receivers and δt is a time window (*King et al.*, 2010).

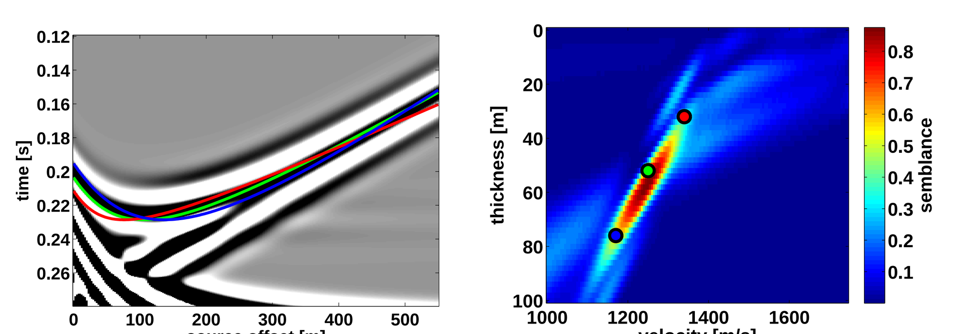

Figure 5: Left: crosscorrelation gather for receiver 101 ∼ 400 m from the virtual source (receiver 1). Right: semblance panel for receiver 1 crosscorrelated with receiver 101. The colored lines in the left plot map to the corresponding dots in the right plot.

The maximum semblance in Figure 5 occurs near the correct velocity and thickness. This example illustrates the non-unique solution for thickness and velocity. We see that many combinations of v_1 and H give similar T_{diff} curves. Next we look at the semblance as separation between receivers decreases.

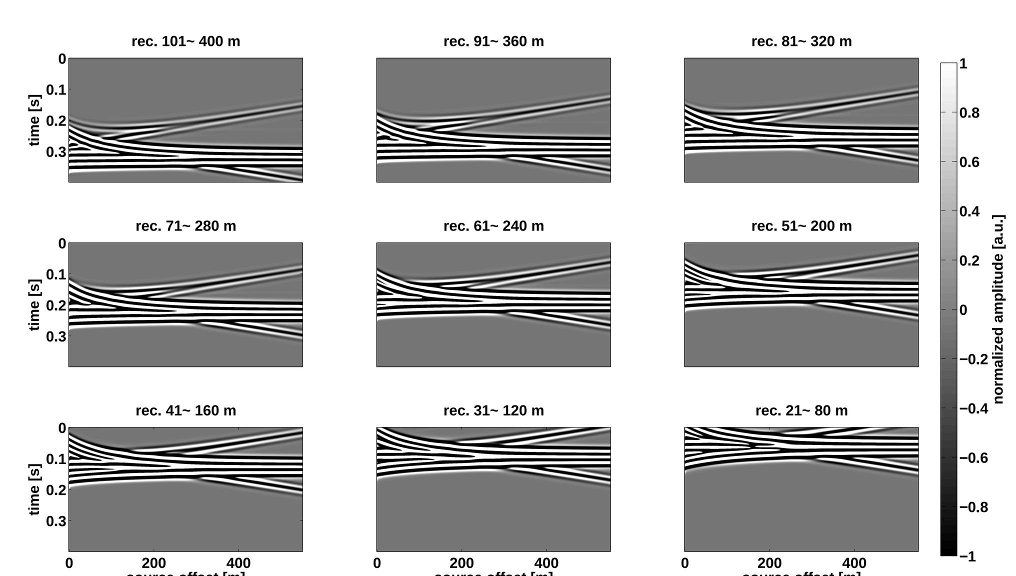

Figure 6: Crosscorrelation gathers for receivers–starting at the maximum offset and moving closer to the virtual shot location.

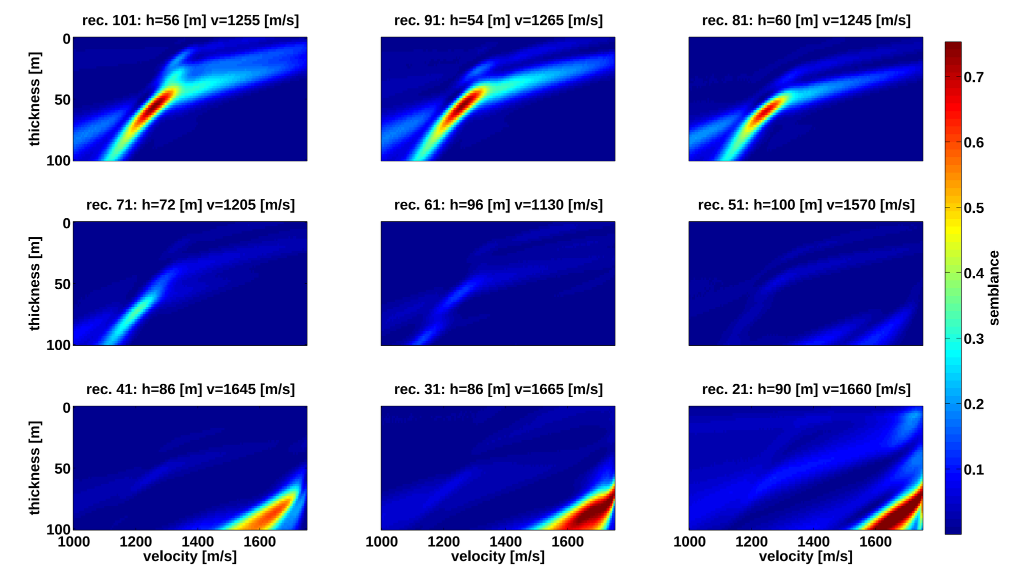

Figure 7: Semblance panels for receivers–starting at the maximum offset and moving closer to the virtual shot location.

Success of the semblance technique depends on the offset between receivers as shown in Figure 7. Note that the correct maximum is not visible at close offsets. This is because the stationary-phase point overlaps in space and time with other stationary points in the crosscorrelation gather. For receivers 21 and 31, we see that the stationary-phase point overlaps with other energy related to the strong direct wave. **The true model is h=50 m and velocity=1250 m/s.** Because the semblance gives the same information for each pair of receivers that we crosscorrelate, we can stack semblance panels together in order to increase the signal-to-noise. This is illustrated in Figure 8

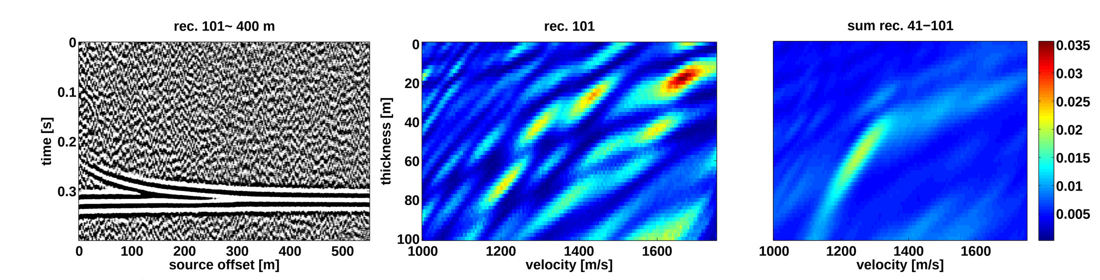

Figure 8: Left: crosscorrelation gather at receiver 101. We add enough noise so that the stationary-phase point is no longer visible by eye. Middle: semblance panel for the single crosscorrelation gather. Right: semblance panel after stacking semblance panels from receivers 41 to 101. Stacking now makes it possible to estimate the thickness and velocity.

A controlled field data example

We acquired a 2D refraction data set at the Boise Hydrogeophysical Research Site (BHRS) to determine water-table depth from the surface and seismic wave velocities. The BHRS is a research well-field near Boise, Idaho (USA), developed to study properties of heterogeneous aquifers using hydrological and geophysical tools (*Barrash et al.*, 1999).

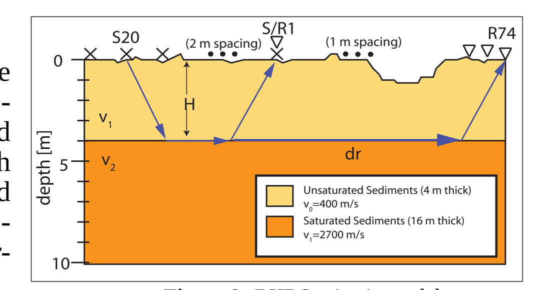

Figure 9: BHRS seismic model.

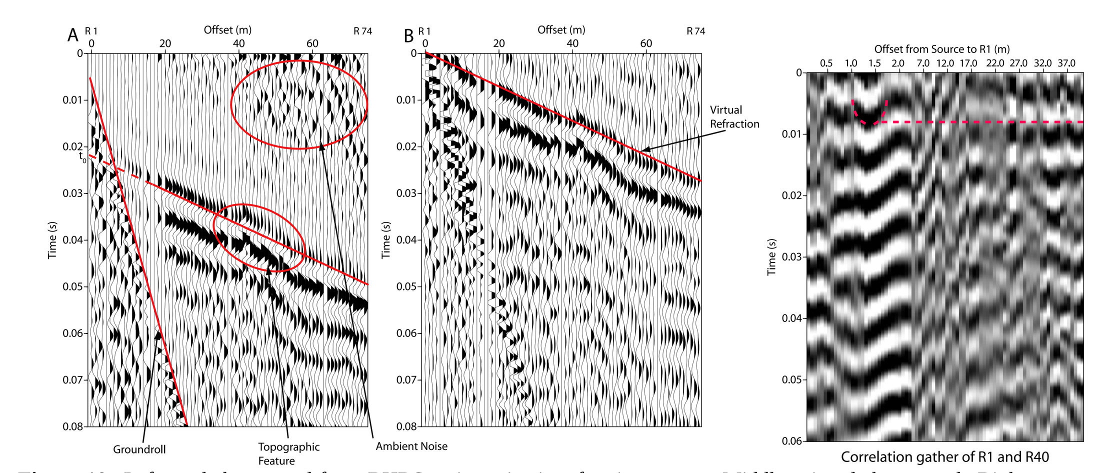

Figure 10: Left: real shot record from BHRS active seismic refraction survey. Middle: virtual shot record. Right: example crosscorrelation gather from *Nichols et al.* (2010).

The virtual refraction is the first arrival in the virtual shot record with estimated velocity near the known saturated sediment velocity. Due to stacking in the interferometric result, we see the ambient noise is suppressed in the virtual shot record. Based on the crosscorrelation gather in Figure 10, it is difficult to estimate the stationary-phase point in the data. In this case, the manual critical offset analysis maybe not the best choice to estimate subsurface parameters. Therefore, we implement semblance analysis to estimate the parameters controlling the stationary-phase point (Figure 12). The complete crosscorrelation is shown in Figure 11 (left) with the theoretical T_{diff} drawn on the right.

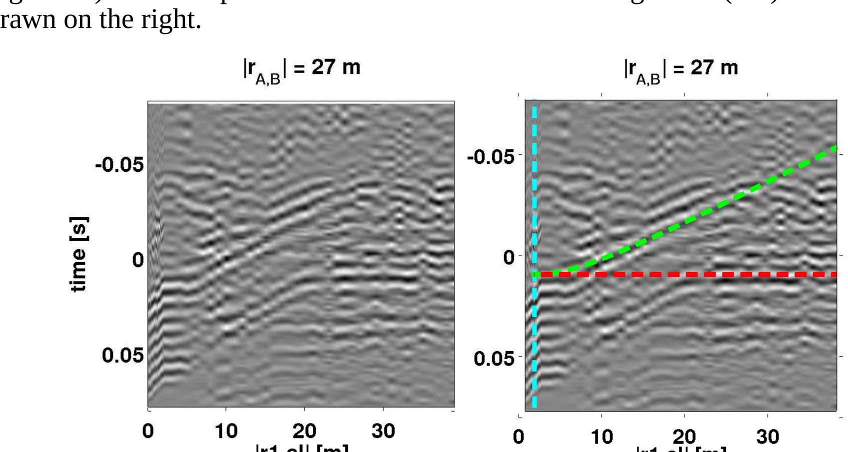

Figure 11: Left: complete crosscorrelation gather at BHRS. Right: same crosscorrelation gather with theoretical T_{diff} curve calculated from the estimated velocities and water-table depth (green). Red and cyan curves are those from Figure 3.

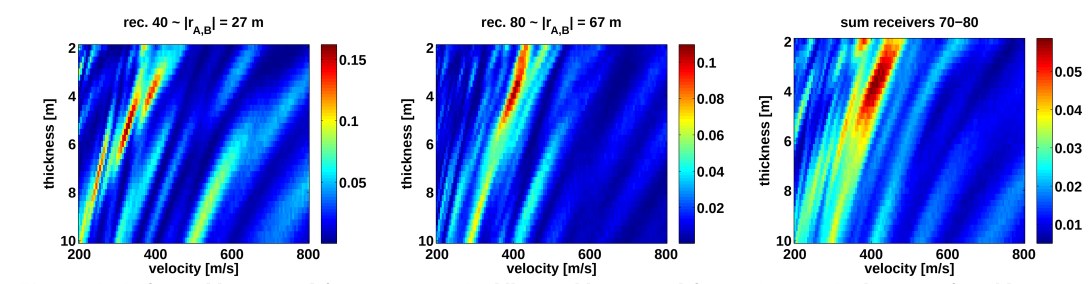

Figure 12: Left: semblance panel for receiver 40. Middle: semblance panel for receiver 80. Right: sum of semblance panels from receivers 70 to 80. The estimated depth to the water-table during data acquisition was 3.9 m and the unsaturated sediment velocity was 400 m/s. The maximum semblance occurs at 3.5 m and 415 m/s in the right semblance panel.

Future work: toward estimating statics

The semblance approach is a robust tool to estimate the slow layer thickness and velocity between the virtual shot position and the source at the critical offset. Because of this, we would like to investigate statics estimation using the virtual refraction analysis. The plots in Figure 13 show a shot record (left) and crosscorrelation gather (right) from a land exploration seismic experiment. A possible stationary-phase point is visible in the right plot; therefore, we believe that we can estimate the weathering layer thickness and velocity along this 2D line.

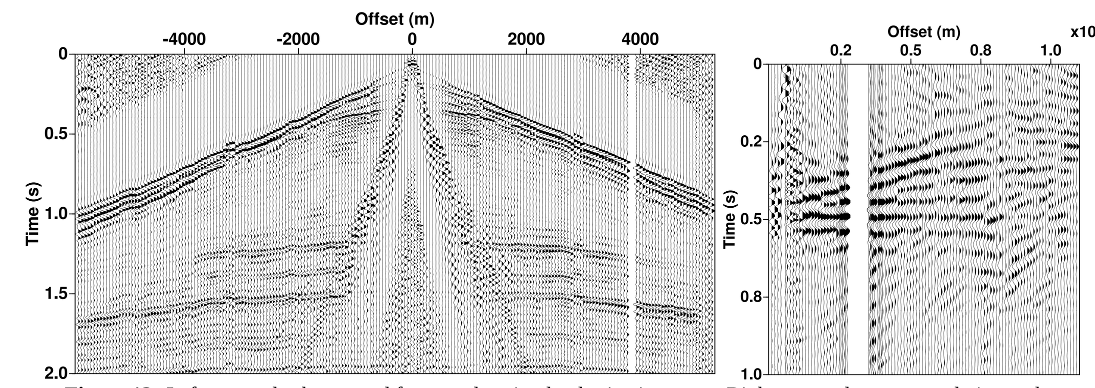

Figure 13: Left: example shot record from exploration land seismic survey. Right: example crosscorrelation gather.

Conclusion

- Spurious head waves in applications of seismic interferometry are often present because requirements for exact recovery of the Green's function between receivers cannot be met in practice.
- We estimate the velocity of the faster layer from the slope of the virtual refraction.
- We estimate the velocity and thickness of the slower layer from semblance analysis of the travel time difference equation (T_{diff}) between reflected energy at the virtual shot location and refracted energy at the other receiver.
- The semblance is sensitive to correctly picking the arrival time of the virtual refraction.
- We need to develop a method to estimate the error in the parameter estimates using the semblance technique.

Acknowledgments

We thank Gabi Melo and Alison Malcolm for help in processing the BHRS data and discussions about semblance. We also thank the developers of SPECFEM2D.

References

Barrash, W., T. Clemo, and M. D. Knoll (1999), Boise hydrogeophysical research site (bhrs): Objectives, design, initial geostatisical results, *Proceedings of SAGEEP99, the Symposium on the Application of Geophysics to Engineering and Environmental Problems*, pp. 389–398.

King, S., A. Curtis, and T. Poole (2010), Interferometric velocity analysis using physical and non-physical energy, in press, Geophysics.

Komatitsch, D., and J.-P. Vilotte (1998), The spectral element method: An efficient tool to simulate the seismic response of 2d and 3d geological structures, *Bull. Seism. Soc. Am.*, *88*(2), 368–392.

Mikesell, D., K. van Wijk, A. Calvert, and M. Haney (2009), The virtual refraction: Useful spurious energy in seismic interferometry, *Geophysics*, *74*(3), A13–A17, doi:10.1190/1.3095659.

Nichols, J., T. D. Mikesell, and K. van Wijk (2010), Application of the virtual refraction to near-surface characterization at the boise hydrogeophysical research site, *Geophysical Prospecting*, *58*(1011–1022).

Snieder, R., K. van Wijk, M. Haney, and R. Calvert (2008), Cancellation of spurious arrivals in Green's function extraction and the generalized optical theorem, *Phys. Rev. E*, *78*, 036,606, doi:10.1103/PhysRevE.78.036606.

Wapenaar, K., and J. Fokkema (2006), Green's function representations for seismic interferometry, *Geophysics*, *71*(4), S133–S146, doi:10.1190/1.2213955.

author email: dmikesell@cgiss.boisestate.edu **AGU FALL MEETING 2010**